International Journal of Abrasive Technology

ISSN online: 1752-265X - ISSN print: 1752-2641
https://www.inderscience.com/ijat

Development of precision analysis method of tooth profile in gear skiving process with shape projection of removal area

Hiroki Yonezawa, Jun'ichi Kaneko, Takeyuki Abe, Naruhiro Irino, Yuta Shinba, Yasuhiro Imabeppu

Article History:
Received:
Accepted:
Published online: 12 February 2025

Development of precision analysis method of tooth profile in gear skiving process with shape projection of removal area

Hiroki Yonezawa*, Jun'ichi Kaneko and Takeyuki Abe

Graduate School of Science and Engineering,
Saitama University,
Shimo-Okubo 255, Sakura-ku,
Saitama-shi, Saitama 338-8570, Japan
Email: h.yonezawa.626@ms.saitama-u.ac.jp
Email: jkaneko@mech.saitama-u.ac.jp
Email: abe@mech.saitama-u.ac.jp
*Corresponding author

Naruhiro Irino, Yuta Shinba and Yasuhiro Imabeppu

DMG MORI Co, Ltd.,
201 Midai, Iga City,
Mie 519-1414, Japan
Email: na-irino@dmgmori.co.jp
Email: yu-shinba@dmgmori.co.jp
Email: ya-imabeppu@dmgmori.co.jp

Abstract: Gear skiving process is gear machining method in which skiving cutter machines a workpiece continuously while rotating synchronously with shaft angle. Gear skiving process is an efficient way to machine internal gears, it has been difficult with conventional machining methods. In the previous studies of gear skiving, a method to derive workpiece removal area from relative motion trajectory of the tool edge surface viewed from workpiece coordinate system is widely used in predicting tooth flank geometry. In this study, a new calculation method of shape projection of removal area viewed from workpiece tooth lead direction is proposed. The proposed method can realise analysis to estimate spur and helical tooth profile. For verification, we also developed tooth profile analysis program using Z-map model, which is same as above method to derive removal area viewed from workpiece coordinate system in previous studies. And we compared the result of calculating shape projection and the result of using Z-map model. As a result, the shape projection of removal area is close to the tooth profile of Z-map model also the tooth profile machined under same conditions as in the analysis. In conclusion, high-precision analysis of tooth flank geometry was achieved.

Keywords: gear skiving; tooth profile; analysis; helical gear; Z-map.

Reference to this paper should be made as follows: Yonezawa, H., Kaneko, J., Abe, T., Irino, N., Shinba, Y. and Imabeppu, Y. (2024) 'Development of precision analysis method of tooth profile in gear skiving process with shape projection of removal area', *Int. J. Abrasive Technology*, Vol. 12, No. 5, pp.1–14.

Biographical notes: Hiroki Yonezawa is a Master course student at Saitama University. His research interests focus on gear machining technology.

Jun'ichi Kaneko received his PhD in Mechanical Engineering from Osaka University, Japan, in 2004. He joined Saitama University in 2004. Since then, he has been engaged in research on simulation of machining processes, CAM algorithms, and optimisation of multi-axis machining operations. Currently, he is a Professor at Saitama University. He is a board member of the Japan Society for Die and Mold Technology, an ISO committee member, and a member of the Japan Society of Mechanical Engineers and the Japan Society for Precision Engineering.

Takeyuki Abe is an Associate Professor at the Graduate School of Science and Engineering at Saitama University. His research focuses on metal additive manufacturing, ranging from the deposition to the simulation process of the wire and arc additive manufacturing method.

Naruhiro Irino received his Doctor degree in Engineering from Chuo University, Japan in 2005. He joined DMG MORI CO. Ltd in 2005. He focuses on the study of machine tools based on deep learning, chatter vibration, sensor-based measurement systems, prediction models for high efficiency machining, and vision-based machine accuracy measurement methods. He is an Executive Officer of DMG MORI and Director of the Advanced Technology Research Center.

Yuta Shinba received his Masters degree in Engineering from Nagoya University, Japan in 2016. He has worked in DMG MORI CO. Ltd since 2019. He specialises in digital twin cutting simulation and works in the Digital Twin Research Center.

Yasuhiro Imabeppu graduated from Kumamoto National College of Technology, Japan in 2007. He joined DMG MORI CO. Ltd in 2007. He specialises in chatter analysis and digital twin cutting simulation. He is the General Manager of the Digital Twin Research Center.

This paper is a revised and expanded version of a paper entitled 'Development of precision analysis method of tooth profile in gear skiving process with shape projection of removal area' presented at The 25th International Symposium on Advances in Abrasive Technology, Evergreen Laurel Hotel, Taichung City, Taiwan, 10–13 December 2023.

1 Introduction

Gear skiving process has been attracting attention in recent years because it enables highly efficient machining of internal gears, which has been difficult with existing machining methods. In the previous studies of gear skiving, A method to derive workpiece removal area from relative motion trajectory of tool edge surface viewed from workpiece coordinate system is widely used (Tachikawa et al., 2015; Ren et al., 2022). Comparing the trajectory of tool edge surface to that passed just before makes it possible to predict tool wear and cutting force by calculating the cut thickness (Jumg et al., 2020; Onozuka et al., 2020). Despite previous research focusing on cutting force prediction and other aspects of the gear skiving process, a method to predict tooth profile after gear skiving process from removal area remains elusive. A method to predict tooth profile by removal area of any tool edge surface is useful for skiving tool design. For example, profile crowning tool, chamfering tool, and not involute curves profile tool can be designed by the method. In addition, the method makes it possible to predict effects of disturbances such as tool wear and mounting angle errors on the tooth profile. CAD-based model and Z-map model are previous methods, but these methods are high computational load because of enormous collision determinations and repeated calculations. This study aims to establish the method to predict tooth profile after gear skiving process in shorter time.

1.1 Specifications used in calculations

m_n is normal module. Z is number of teeth. α_n is normal pressure angle on the pitch circle. β is helix angle. The subscript 't' is the specification of the tool, and 'w' is the specification of the workpiece.

1.2 Overview of skiving process

Figure 1 shows a schematic diagram of gear skiving. Gear skiving process is gear machining method in which skiving tool machines a workpiece continuously while rotating synchronously with fixed shaft angle. The skiving tool processes a workpiece while progressing at a tool feed rate f_t.

Figure 1 Schematic diagram of gear skiving (see online version for colours)

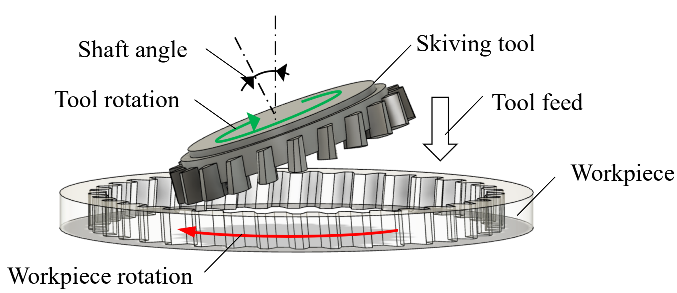

2 Calculating relative motion of skiving tool on workpiece coordinate system

2.1 Tool and workpiece position relationship

Figure 2 shows a schematic diagram of tool coordinate system and workpiece coordinate system. Workpiece coordinate system (x_w, y_w, z_w) is set at the centre of workpiece rotation. An origin of z_t is a position where tool and workpiece are tooth aligned first. If addendum modification is not considered, A distance L between the origin of tool coordinate system and workpiece coordinate system, which is the difference between workpiece axial pitch circle radius Rp_w and tool axial pitch circle radius Rp_t, is final cut-in position [see equations (1), (2) and (3)]. The origin of tool coordinate system is set at (L, 0, Z″) on workpiece coordinate system (Z″ is optional z_w coordinate).

$$Rp_t = m_n Z_t / \cos(\beta_t)/2. \tag{1}$$

$$Rp_w = m_n Z_w / \cos(\beta_w)/2. \tag{2}$$

$$L = Rp_w - Rp_t. \tag{3}$$

2.2 *Relative motion of skiving tool on workpiece coordinate system*

If skiving tool tip is on x_w-axis of workpiece coordinate system (shown in Figure 2), rotational motion of skiving tool and workpiece can be considered as a two-dimensional motion in $y_w z_w$-plane. Figure 3 shows a relative motion of skiving tool and workpiece at an instant when skiving tool tip passes over workpiece coordinate system xw-axis. The skiving tool is tilted by shaft angle Σ to mesh with normal profile of workpiece. The relative motion of skiving tool follows workpiece lead direction. Equation (4) shows relationship between tool helical angle and workpiece helical angle (Jumg et al., 2020).

$$\beta_w = \Sigma - \beta_t. \tag{4}$$

Figure 2 Schematic diagram of tool coordinate system and workpiece coordinate system (see online version for colours)

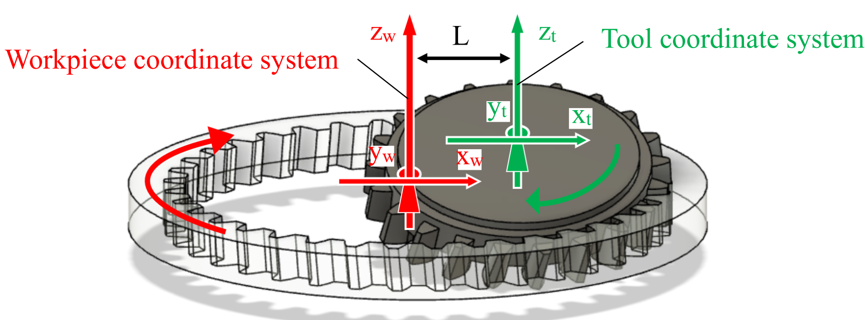

Equation (5) shows tool peripheral velocity V_t, and equation (6) shows workpiece peripheral velocity V_w.

$$V_t = Rp_t \omega_t. \tag{5}$$

$$V_w = Rp_w \omega_w. \tag{6}$$

Figure 3 Schematic diagram of relative vector of tool and workpiece

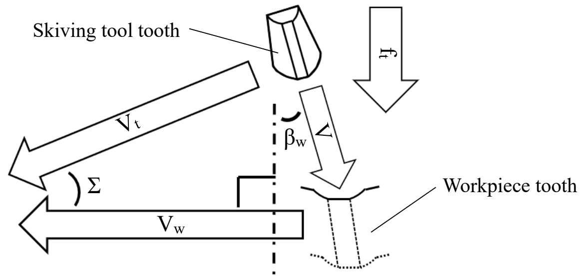

Equation (7) shows an equilibrium equation in tool feed direction from equations (5) and (6). Similarly, equation (8) shows an equilibrium equation in workpiece rotation direction (V is the relative velocity of tool edge surface as viewed from workpiece).

$$V\cos(\beta_w) = V_t \sin(\Sigma) + f_t. \tag{7}$$

$$V_w = V_t \cos(\Sigma) + V\sin(\beta_t). \tag{8}$$

By eliminating the relative velocity V in equations (7) and (8), equation (9) shows an equation relating angular velocity of skiving tool and workpiece.

$$\omega_w = Z_t / Z_w \, \omega_t + 2f_t \sin(\beta_w) / (m_n Z_w). \tag{9}$$

Figure 4 Coordinate transformation from tool coordinate system to workpiece coordinate system (see online version for colours)

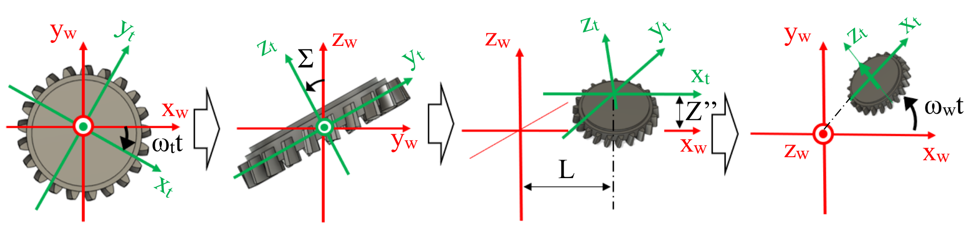

In the coordinate system shown in Figure 2, relative motion of tool edge surface as viewed from workpiece coordinate system is calculated. Figure 4 shows coordinate transformation from tool coordinate system to workpiece coordinate system. Skiving tool is rotating around tool coordinate system z_t-axis, and z_t-axis is tilted by shaft angle Σ with z_w-axis of workpiece coordinate system. Tool coordinate system is translational to (L, 0, Z″) on workpiece coordinate system and orbits around z_w-axis in opposite direction of workpiece rotation. Equation (10) shows the coordinate transformation matrix M_t that transforms from tool coordinate system (x_t, y_t, z_t) to workpiece coordinate system (x_w, y_w, z_w) (Tachikawa et al., 2015).

$$M_t = \begin{bmatrix} \cos(\omega_w t) & -\sin(\omega_w t) & 0 & 0 \\ \sin(\omega_w t) & \cos(\omega_w t) & 0 & 0 \\ 0 & 0 & 1 & 0 \\ 0 & 0 & 0 & 1 \end{bmatrix} \begin{bmatrix} 1 & 0 & 0 & L \\ 0 & 1 & 0 & 0 \\ 0 & 0 & 1 & Z'' - f_t t \\ 0 & 0 & 0 & 1 \end{bmatrix} \begin{bmatrix} 1 & 0 & 0 & 0 \\ 0 & \cos(\Sigma) & -\sin(\Sigma) & 0 \\ 0 & \sin(\Sigma) & \cos(\Sigma) & 0 \\ 0 & 0 & 0 & 1 \end{bmatrix} \begin{bmatrix} \cos(-\omega_t t) & -\sin(-\omega_t t) & 0 & 0 \\ \sin(-\omega_t t) & \cos(-\omega_t t) & 0 & 0 \\ 0 & 0 & 1 & 0 \\ 0 & 0 & 0 & 1 \end{bmatrix}. \tag{10}$$

3 Definition of tool edge surface

3.1 Involute curve

In the previous study, a skiving tool was defined by generating a shape with a grinding wheel formed into rack shape (Uriu et al., 2017). In this study, a point cloud of tool edge surface (x_t, y_t, z_t) in tool coordinate system is defined as intersections of a helical gear and rake face (the helical gear is same as target workpiece normal module), ignoring effects of side clearance angle and front clearance angle. Figure 5 shows involute curves constituting tool edge surface. An involute curve has a property that a tangent at any point on the curve is orthogonal to a tangent drawn from that point to the base circle (Ishikawa, 2022).

Figure 5 Involute curves on tool coordinate system (see online version for colours)

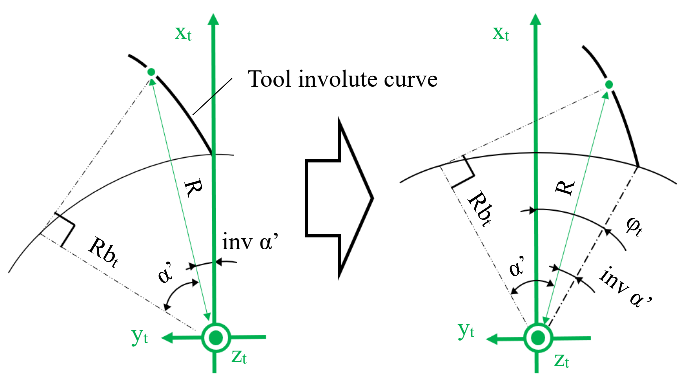

Equation (11) shows tool axial pressure angle on the pitch circle α_t, equation (12) shows tool axial base circle radius Rb_t, equation (13) shows pressure angle α' at any point on involute curve, equation (14) shows an angle $inv\alpha'$ between x_t-axis and a straight line connecting any point on involute curve and the origin of tool coordinate system, equation (15) shows range of parameter R (Ra_t is tool tip circle radius).

$$\alpha_t = a\tan\left(\tan(\alpha_n)/\cos(\beta_t)\right). \tag{11}$$

$$Rb_t = Rp_t \cos(\alpha_t). \tag{12}$$

$$\alpha' = a\cos\left(Rb_t/R\right). \tag{13}$$

$$\mathrm{inv}\alpha' = \tan(\alpha') - \alpha'. \tag{14}$$

$$Rb_t <= R <= Ra_t = Rp_t + 1.25m_n. \tag{15}$$

Equations (16) and (17) shows axial involute curves in tool coordinate system.

$$x_t''' = R\cos(\mathrm{inv}\alpha'). \tag{16}$$

$$y_t''' = R\sin(\mathrm{inv}\alpha'). \tag{17}$$

Equation (18) shows an amount of rotation φ_t to make tool tooth tip come on x_t-axis (Senba, 1959).

$$\varphi_t = \pi/(2\,Z_t) + \tan(\alpha_t) - \alpha_t. \tag{18}$$

Equations (19) and (20) shows axial involute curves with tooth tip on x_t-axis.

$$x_t'' = x_t'''\cos(-\varphi_t) - y_t'''\sin(-\varphi_t). \tag{19}$$

$$y_t'' = x_t'''\sin(-\varphi_t) + y_t'''\cos(-\varphi_t). \tag{20}$$

3.2 Helical gear

A helical gear is arranged as strings with a constant helix angle β_t on axial pitch circle (shown in Figure 6). Equation (21) shows relationship between an amount of rotation around z_t-axis at each z_t position and tooth width H, equation (22) shows a minute amount of rotation around z_t-axis per z_t position (Nakada, 1969).

$$\theta_t = H\tan(\beta_t)/Rp_t. \tag{21}$$

$$d\theta_{t,z} = \tan(\beta_t)/Rp_t. \tag{22}$$

Equations (23), (24) and (25) shows a point cloud of helical gear as source of tool edge surface (Z' is any z_t position).

$$z_t' = Z'. \tag{23}$$

$$x_t' = x_t''\cos\left(d\theta_{t,z}Z'\right) - y_t''\sin\left(d\theta_{t,z}Z'\right). \tag{24}$$

$$y_t' = x_t''\sin\left(d\theta_{t,z}Z'\right) + y_t''\cos\left(d\theta_{t,z}Z'\right). \tag{25}$$

3.3 Intersections of helical gear and rake face

Figure 7 shows intersections of helical gear and rake face in tool coordinate system constructed by equations (23), (24) and (25). The rake face is defined by rake angle γ and mounting angle σ. Equation (26) shows a vector perpendicular to rake angle inclined by mounting angle in tool coordinate system.

$$(i_t, j_t, k_t) = \left(\sin(\gamma), \cos(\gamma), \sin(\sigma), \cos(\gamma), \cos(\sigma)\right). \tag{26}$$

Figure 6 An amount of rotation around z_t-axis at each z_t position in helical gear (see online version for colours)

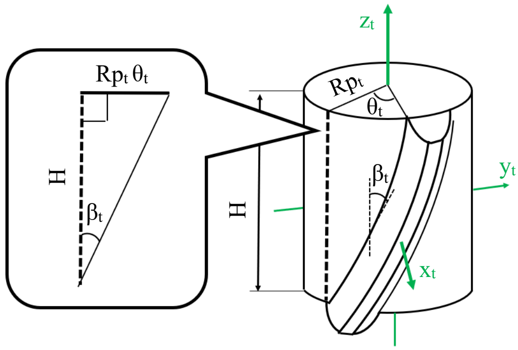

Equation (27) shows an equation of a plane perpendicular to the vector in equation (26) and passing through coordinates of tool tip (Ra_t, 0, 0).

$$\sin(\gamma)(x_t - Ra_t) + \cos(\gamma)\sin(\sigma)y_t + \cos(\gamma)\cos(\sigma)z_t = 0. \tag{27}$$

A point $(x'_{t,n}, y'_{t,n}, z'_{t,n})$ is any point satisfying equations (23), (24) and (25). A point $(x'_{t,n+1}, y'_{t,n+1}, z'_{t,n+1})$ satisfying equations (23), (24) and (25) has the same parameter R as $(x'_{t,n}, y'_{t,n}, z'_{t,n})$. $z'_{t,n+1}$ has a distance d_z from $z'_{t,n}$. Equations (28) and (29) shows an equation of a line connecting $(x'_{t,n}, y'_{t,n}, z'_{t,n})$ and $(x'_{t,n+1}, y'_{t,n+1}, z'_{t,n+1})$.

$$(x_t - x'_{t,n})/(x'_{t,n+1} - x'_{t,n}) = (y_t - y'_{t,n})/(y'_{t,n+1} - y'_{t,n}). \tag{28}$$

$$(y_t - y'_{t,n})/(y'_{t,n+1} - y'_{t,n}) = (z_t - z'_{t,n})/(z'_{t,n+1} - z'_{t,n}). \tag{29}$$

The points (x_t, y_t, z_t), which is solutions of equations (27), (28) and (29) and satisfies $z'_{t,n} <= z_t <= z'_{t,n+1}$, is defined as a point cloud of tool edge surface in tool coordinate system.

4 Analysis of tooth profile by shape projection

4.1 Calculating removal area

From the coordinate transformation [equation (10)] and the point cloud of tool edge surface [equations (27), (28) and (29)], equation (30) shows coordinates of tool edge surface in workpiece coordinate system (Tachikawa et al., 2015).

$$\begin{bmatrix} x_w \\ y_w \\ z_w \\ 1 \end{bmatrix} = M_t \begin{bmatrix} x_t \\ y_t \\ z_t \\ 1 \end{bmatrix}. \tag{30}$$

Removal area (see in Figure 8), the area through which tool edge surface has passed along the relative motion, can be calculated by calculating equation (30) in range from a time when the tool tip interferes with workpiece to a time t when it no longer interferes with workpiece. Workpiece tooth flank can be considered as the shape of multiple removal areas aligned in workpiece lead direction.

Figure 7 Intersections of helical gear and rake face (see online version for colours)

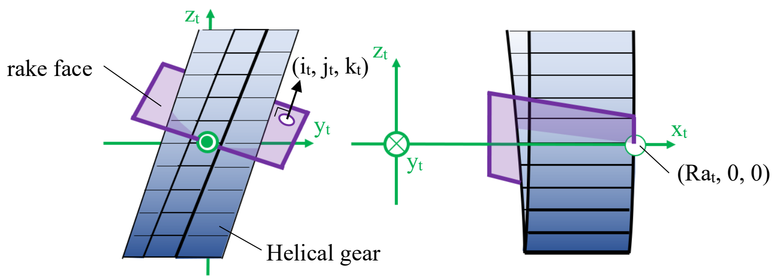

Figure 8 Removal area (see online version for colours)

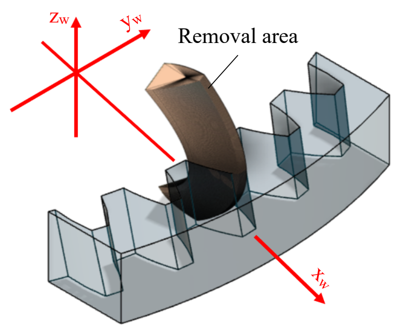

4.2 *Analysis method by shape projection*

Figure 9 shows a method of analysing tooth profile predicted from a projected shape of the removal area in z_w-axis direction. When analysing tooth profile of helical gear by shape projection, the tooth profile cannot be compared with the projected shape by simply observing the removal area from z_w-axis direction because tooth profile is twisted in z_w-axis direction. Therefore, the point cloud of removal area was rotated by an amount of rotation around z_w-axis for each z_w position by workpiece helical angle β_w. This makes it possible to align workpiece axial tooth profile and the removal area in z_w-axis direction. Equation (31) shows an amount of rotation around z_w-axis by a distance in z_w-axis direction from the origin of workpiece coordinate system (Nakada, 1969).

$$d\theta_{w,z} = \tan(\beta_w)/Rp_w. \tag{31}$$

Equations (32) and (33) shows a point cloud of removal area aligned in z_w-axis direction.

$$x'_w = x_w \cos(d\theta_{w,z} z_w) - y_w \sin(d\theta_{w,z} z_w). \tag{32}$$

$$y'_w = x_w \sin(d\theta_{w,z} z_w) + y_w \cos(d\theta_{w,z} z_w). \tag{33}$$

Figure 9 A method of analysing tooth profile predicted by shape projection (see online version for colours)

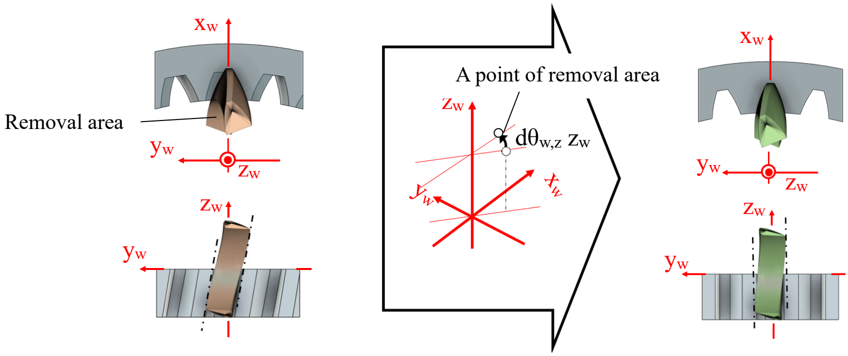

4.3 *A method of evaluating analysis results*

Figure 10 shows a method for evaluating analysis results. The largest and smallest point cloud in y_w-direction is extracted from the projected shape of removal area. A 10th-order approximation for each of the largest and smallest point cloud in y_w-direction is derived. A distance from R position of target workpiece axial tooth profile to the approximate curve of the projected shape in normal direction of the R position is defined as profile deviation (target workpiece axial tooth profile is calculated in the same way as in equations (11)–(20) (Tachikawa et al., 2015; Uriu et al., 2017).

Figure 10 A method for evaluating analysis results (see online version for colours)

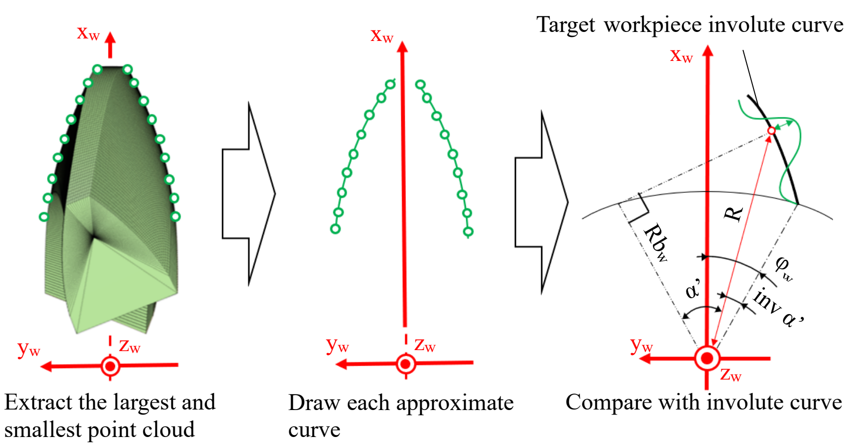

5 Analysis using Z-map model

5.1 *Tooth profile and uncut length*

Tooth profile analysis using Z-map model was performed to compare the results with shape projection analysis results. Figure 11 shows workpiece Z-map model. Workpiece axial tooth profile is placed at each z_w position while rotating it by the amount of rotation for each z_w position in equation (31). An angle of x'_w -axis with x_w-axis is same as the angle of rotation according to equation (31). Uncut length (see in Figure 11) is the remaining quantity from target tooth profile. The uncut length is defined as a vector with the length from tooth profile coordinates to workpiece tooth tip circle in same direction as the x'_w -axis at its z_w position.

Figure 11 Z-map model and uncut length (see online version for colours)

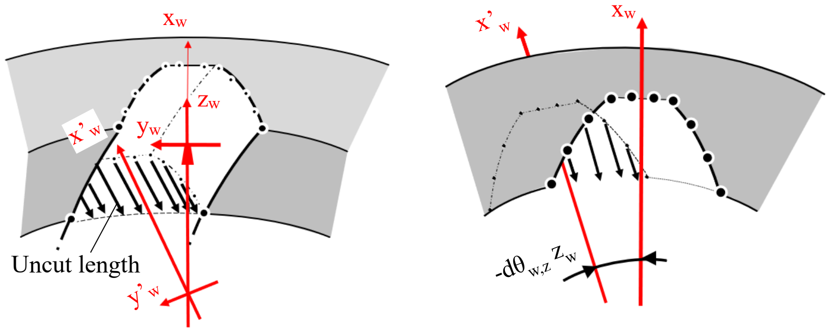

5.2 Updating uncut length

Uncut length is updated by using the point cloud of removal area for collision determination (Figure 12). If uncut length interferes with interior of the $y'_w z'_w$ plane at any three points in the removal area calculated by equation (30), the intersections of uncut length with the plane constituted by those three points is calculated. A length from the intersections to the beginning of uncut length is defined as new uncut length. This process is repeated until the skiving tool is completely passed through the workpiece by tool feed.

Figure 12 Updating uncut length by using removal area (see online version for colours)

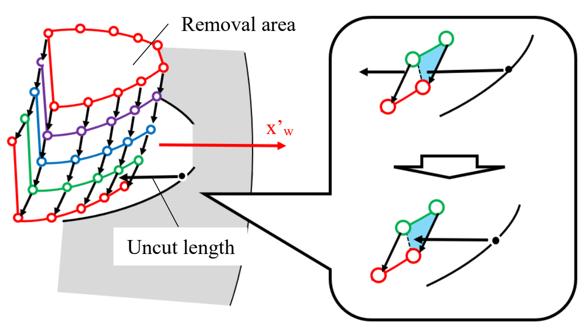

5.3 A method of evaluating Z-map analysis results

Figure 13 shows an evaluation method of analysis results by Z-map model. Coordinates of a tip of uncut length after Z-map analysis are used as tooth profile of the analysis result. As in the case of predicting tooth profile by shape projection, a 10th-order approximation formula was derived for the coordinates of a tip of uncut length, and a distance between the approximation curve and target tooth profile was defined as profile deviation.

Figure 13 A method for evaluating Z-map analysis results (see online version for colours)

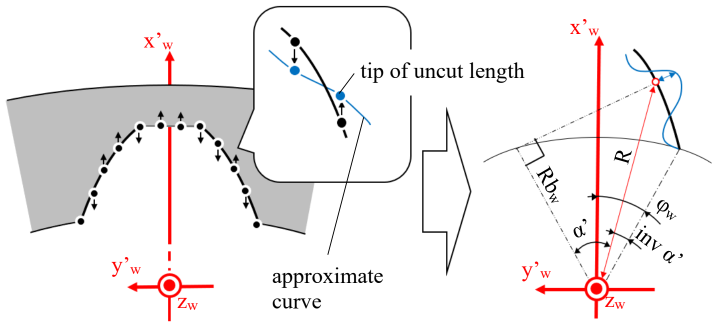

6 Comparison of analysis results

6.1 Analytical specification

Table 1 shows specifications of tooth profile analysis in gear skiving process. Normal module and normal pressure angle of target tooth profile are same as the tool specifications. Using Table 1 specifications, equations (1)–(33) are calculated, and the analysis is performed using the shape projection and the Z-map model.

Table 1 Specifications of tooth profile analysis

Tool specifications	
Normal module m_n [mm]	2.000
Normal pressure angle α_n [deg]	20.000
Number of teeth Z_t [–]	25
Helix angle (right-hand) β_t [deg]	5.000
Mounting angle σ [deg]	5.000
Rake angle γ [deg]	0.000
Number of points [–]	1024
Target workpiece specifications	
Number of teeth (internal) Z_w [–]	41
Helix angle (left-hand) β_w [deg]	15.000
Number of points	512
Mechanical specifications	
Tool feed rate f_t [mm/s]	1.333
Shaft angle Σ [deg]	20.000
Tool angular velocity ω_t [rpm]	655.934
Step size of t [–]	10^{-5}

6.2 Analysis results

Figures 14 and 15 shows comparison of the analysis results obtained by shape projection with target tooth profile, and comparison the analysis results obtained by Z-map analysis with target tooth profile. The vertical axis is R position of target tooth profile, and the horizontal axis is profile deviation at the R position. A point on the + side of horizontal axis indicates that the workpiece profile is thicker than target tooth profile, and a point on the – side of the horizontal axis indicates that the workpiece profile is thinner than target tooth profile.

Figure 14 The result of workpiece left tooth profile analysis (see online version for colours)

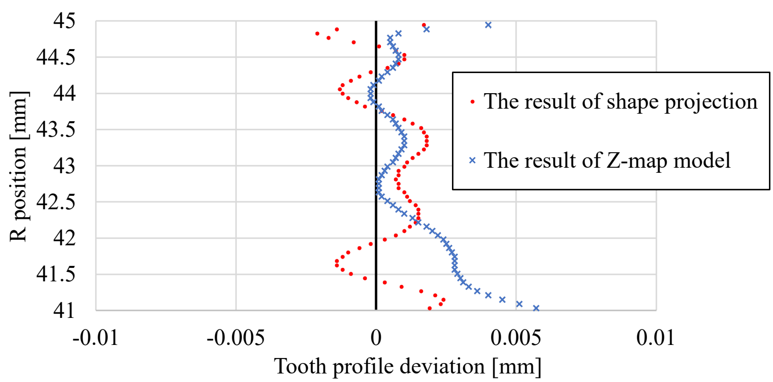

Figure 15 The result of workpiece right tooth profile analysis (see online version for colours)

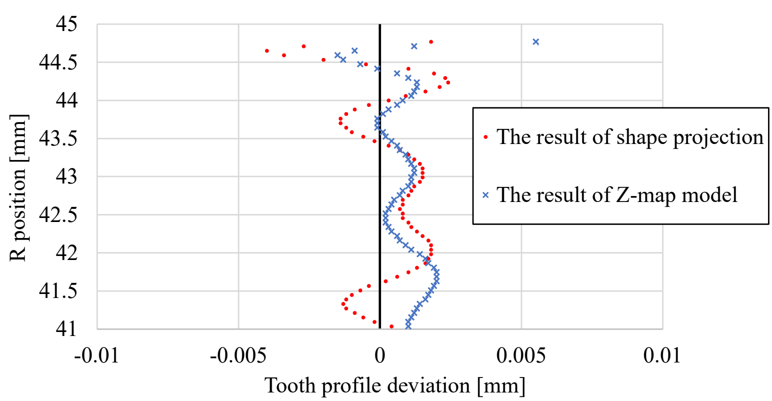

6.3 Consideration of analysis results

Figures 14 and 15 shows that the trends are in good agreement when comparing the results of two analyses. Since the Z-map model analysis is based on actual processing, the shape projection analysis was shown to be effective. While tool marks caused by tool feed rate also affect tooth profile shape in the Z-map analysis, the shape projection analysis can calculate a constant and maximum shape in the tooth profile direction regardless of feed rate. This makes it possible to accurately estimate tooth profile in the skiving process analysis.

Calculation time of shape projection is 0.811 [s], and that of Z-map model is 146.387 [s]. In addition, shape projection is performed with single processing, and Z-map model is performed with 16 parallel processing. The results show that shape projection requires lower computational load and shorter calculation time.

7 Conclusions

- By correcting for an amount of rotation around z_w-axis due to workpiece helical angle, it is possible to estimate tooth profile with projected shape of removal area by simply observing removal area from z_w-axis direction.
- The analysis results of tooth profile estimation method using shape projection agreed well with Z-map analysis results. And the method of shape projection can calculate a constant and maximum shape in the tooth profile direction.
- The shape projection requires lower computational load and shorter calculation time than a method that require enormous collision determinations and repeated calculations.

References

Ishikawa, M. (2022) *Introduction to Gear Cutting*, 1st ed., TAIGA Publishing Co., Ltd., Japan.

Jumg, H., Hayasaka, T., Jang, S. and Shamoto, E. (2020) *Research on Cutting Force Prediction in Gear Skiving, Grantees in Research and Developments in 2020*, MAZAK Foundation, Japan, No. 1.

Nakada, T. (1969) *Gear Synopsis (Haguruma Binran)*, 2nd ed., The Nikkan Kogyo Shimbun, Ltd., Japan.

Onozuka, H., Tayama, F., Yu, H. and Inui, M. (2022) 'Cutting force model for power skiving of internal gear', *Journal of Manufacturing Processes*, Vol. 56, No. Part B, pp.1277–1285.

Ren, Z., Fang, Z., Kizaki, T., Feng, Y., Nagata, T., Komatsu, Y. and Sugita, N. (2022) 'Understanding local cutting features affecting surface integrity of gear flank in gear skiving', *International Journal of Machine Tools & Manufacture*, Vol. 172, pp.1–18.

Senba, M. (1959) *Gear (Haguruma)*, 5th ed., The Nikkan Kogyo Shimbun, Ltd., Japan.

Tachikawa, T., Kurita, N., Nakamura, M. and Moriwaki, I. (2015) 'Study on the skiving process of an internal gear (effects of axial feed rate on gear accuracy)', *Transactions of the JSME*, Vol. 81, No. 831, pp.15–00105.

Uriu, K., Osafune, T. and Moriwaki, I. (2017) 'Study on design of taper shaped skiving cutters for internal gears (taper shaped cutter ground with trapezoidal wheels used for pinion cutter grinding)', *Transactions of the JSME*, Vol. 83, No. 853, pp.17–00156.